Indian Journal of Chemical Technology
Vol. 31, January 2024, pp. 20-25
DOI: 10.56042/ijct.v31i1.5844

Synthesis and characterization of zinc aluminophosphate for catalytic applications

Sreenivasulu Peta* & Shailesh Kumar Mishra
Faculty of Chemical Sciences, Institute of Natural Sciences, Shri Ramswaroop Memorial University, Barabanki, 225 003, U.P, India
*E-mail: sreenivas.chm@srmu.ac.in

Received 26 September 2023; accepted 12 December 2023

In this study, we report a simple method for the synthesis of zinc aluminophosphate ($ZnAlPO_4$) nanoparticles possessing stable possessing ANA-zeotype and LEV crystalline structures. The synthesised nanoparticles exhibit considerable catalytic activity towards selective hydroxylation of toluene. The LEV structures are obtained by hydrothermal synthesis at 150–170 °C, while the ANA structure is obtained just by a simple room-temperature mixing of the ingredients. The synthesised ANA-zeotype nanoparticles exhibit considerable catalytic activity towards selective hydroxylation of toluene.

Keywords: Aluminum phosphate, Catalysis, Hydrothermal synthesis, TPABr, Toluene hydroxylation, Zinc Aluminophosphate

Introduction

Aluminophosphate is a rich variety of microporous structure, including 18 analogues of zeolites. However, the neutral framework charge obtained by the presence of Al^{+3} and P^{+5} limits the materials' applications in catalysis due to their non-acidic nature. Replacement of the framework of Al^{+3} and P^{+5} ions by divalent metal cations such as Mg, Co, and Zn or silicon produces the MAlPO and SAPO family materials[1], which show properties of zeolite like ion-exchange applications, magnetism, acid-catalyzed reactions, and photoluminescence[2-5]. Quantity of heteroatoms with lower valence into AlPO, influences the creation of acid sites and framework stability. Yet, the introduction of more heteroatoms into the framework creates structural instability in the material, and stability decreases as the amount of heteroatoms increases[6]. In most cases, AlPO and MAlPO materials are commonly synthesized in hydrothermal conditions by using different structure-directing agents that are particular to each type of material. Heteroatom-containing aluminophosphates are unstable after the removal of structure-directing agents in many cases, which greatly limits their applications in catalysis and adsorption. Synthesis of the thermally stable MAlPO materials by using novel structure-directing agents, where host-guest charge density[7,8] and fluoride ions are worked as structure-directing agents along with organic amines to facilitate the formation of some special cage structure, such as a double 4-ring, and to compensate for changes in the frame work[9,10].

LEV zeotype minerals were first discovered in 1959; literally, up to now, only four LEV Zeotype aluminophosphate with heteroatoms has been reported, such as SAPO-35[(Ref. 11,12)], CoDAF-4[(Ref.13)], ZnAPO-35[(14)], and MgAlPO [(Ref.15)], by using the following cycloamines, such as tropine, 2-methyl-cyclohexylamine, 1,4-diazabicyclo [2.2.2]octane, quinuclidine, N,N-dimethylpiperidine chloride, 1,2-diaminocyclohexane ($C_6H_{14}N_2$, DACH), and n-methylpiperidine ($C_6H_{13}N$), etc., as structure-directing agents (SDAs). Most of the methods used harsh reaction conditions and templates.

Metal-supported materials are gaining attention due to unique characteristics such as reduced diffusion path length that generally contribute to their improved properties in catalysis and adsorption applications. But there is a lack of information in the literature for the preparation of zinc-incorporated AlPO nanoparticles. We synthesized zinc incorporating AlPO in recent years by using tetrapropylammonium bromide (TPABr) and fluoride as templates and co-templates[16,17]. Here we have synthesized the $ZnAlPO_4$ material possessing ANA-zeotype and LEV crystalline structures. The LEV structures are obtained by hydrothermal synthesis at 150–170 °C, while the ANA structure is obtained just by a simple room-temperature mixing of the ingredients.

Experimental Section

Synthesis

The typical synthesis method involves the dispersion of aluminum nitrate and zinc nitrate powders in a solution of ammonium orthophosphate with vigorous

stirring at room temperature, followed by the sequential addition of tetrapropyl ammonium bromide and hydrofluoric acid, leaving the resultant mixture under stirring for one hour to obtain a homogeneous gel with an overall molar composition of $0.11Al_2O_3$: $0.012Zn:0.36P_2O_5:0.0018SDA:0.11HF$. The obtained resultant gel is processed by two different methods. (i) By adding a few drops of ammonia at room temperature, the white precipitate obtained was filtered, washed with an abundant amount of deionized water, and dried at room temperature overnight, followed by calcinations for 5 hours at 500°C. The samples obtained before and after calcination are denoted as RT and RTC, respectively. (ii) The obtained gel was introduced into Teflon-lined stainless steel autoclaves and heated statically at two different conditions: 150°C and 170°C for 24 h, followed by their calcinations at 500°C for 5 h. The samples synthesized by hydrothermal treatment at 150°C are denoted as HT1 and HT1C, representing before and after calcination, respectively. Similarly, the samples synthesized by hydrothermal treatment at 170°C are denoted as HT2 and HT2C, representing the materials before and after calcination, respectively.

Hydroxylation reaction

The hydroxylation reaction was carried out in a round-bottom flask under reflux conditions with constant cold water flow and constant stirring. In a typical reaction study, 1 mL of toluene, 5 mL of acetonitrile, and 50 mL of catalyst were taken in a round bottom flask, followed by the addition of 5 mL of 50% H_2O_2 in a drop-wise manner. The temperature then increased up to 70°C, and this temperature was maintained for 4 h. The reaction mass was then cooled out, and the product was collected by filtration and analyzed by GC/MS. The performance of the catalyst after three reaction cycles was also evaluated, where the catalyst was separated by filtration and dried at 100°C.

Characterization

Powder X-ray diffraction patterns of the samples were recorded on a Regaku Dmax III B equipped with a rotating anode and CuKα radiation. SEM images were recorded to obtain particle morphology on the Quanta 200f instrument in the Netherlands. The IR spectra of both samples were recorded on the Thermonicolate 8700 instrument, Thermoscientific Corporation, USA.

Results and Discussion

The X-ray diffraction patterns of $ZnAlPO_4$ samples shown in Fig. 1 indicate that the room-temperature synthesized sample (RT) exhibits an ANA zeo-type crystalline structure that retains even after the removal of the template by calcination (RTC) and supports the structural stability of the material. However, the other two materials synthesized by hydrothermal treatment (HT1 and HT2) exhibit LEV zeo-type crystalline structures, and after calcinations, they form semi-crystalline materials, and some of the XRD peaks disappear (HT1C and HT2C). Generally, the LEV structure is known for its structural instability and collapses immediately after the removal of the structure-directing agent.

The structural identity of $ZnAlPO_4$ samples has been confirmed by FTIR spectra (Fig. 2). The samples exhibited the featured vibrational bands associated with the $[PO_4]^{3-}$unit (1127, 504 cm^{-1}), Al (748 cm^{-1})[18], and the two bands obtained at 1009 and 990 cm^{-1} relegated to the vibrations of Zn-O-P[19,20]. The

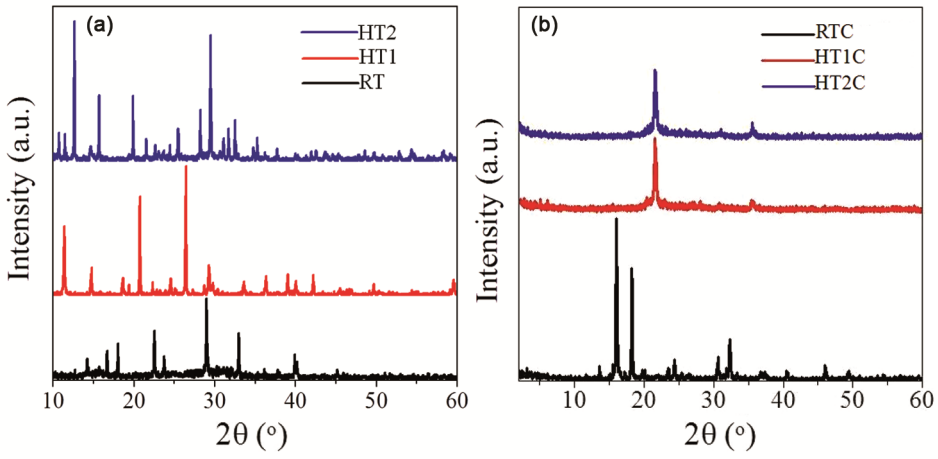

Fig. 1 — Wide angle XRD patterns of $ZnAlPO_4$ samples, (a) before calcination and (b) after calcinations

additional bands observed in the samples before calcination (which disappeared after calcination) are related to the stretching vibrations of the SDA. The EDX analysis (Fig. 3) also confirms the presence of zinc, alumina, and phosphorous species in the samples.

SEM images of all the $ZnAlPO_4$ samples before and after calcination are shown in Fig. 4, where the sample synthesized at room temperature (RT) exhibits spherical morphology before and after calcination (RTC). The hydrothermally synthesized samples HT, HT1C HT2, and HT2C exhibit bunches of flake-like structures with 1 µm size. Overall, the SEM results indicate the difference in structural morphology of the $ZnAlPO_4$ samples synthesized at three different conditions, but the structure morphology is retained after the calcination. The XRD, FT-IR, and TEM envision the presence of Zn in two forms: cystalline $ZnAlPO_4$ and dispersed Zn particles on the $ZnAlPO_4$. The presence of bivalent Zn in the cystalline framework of $AlPO_4$ created the acidity, which is measured by the TPD of ammonia. As shown in Fig. 5, among the three samples, the RTC sample with the ANA phase exhibited higher acidity. The structural stability of the $ZnAlPO_4$ samples is also confirmed by the TGA analysis (Fig. 6), where the synthesized samples revealed a weight loss of 70–140°C related to the desorption of sorbed water and a high temperature weight loss of up to 440°C related to the decomposition of organic template [21]. There is no further weight loss observed above 450°C.

The $ZnAlPO_4$ with ANA-zeotype exhibits both acidity and metal function due to the presence of Zn. Hence, the material is expected to exhibit catalytic

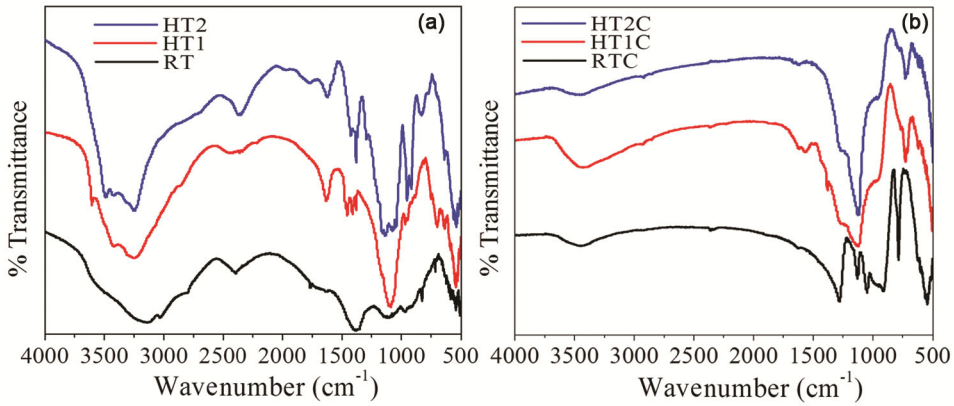

Fig. 2 — FT-IR spectra of $ZnAlPO_4$ samples (a) before calcination and (b) after calcinations

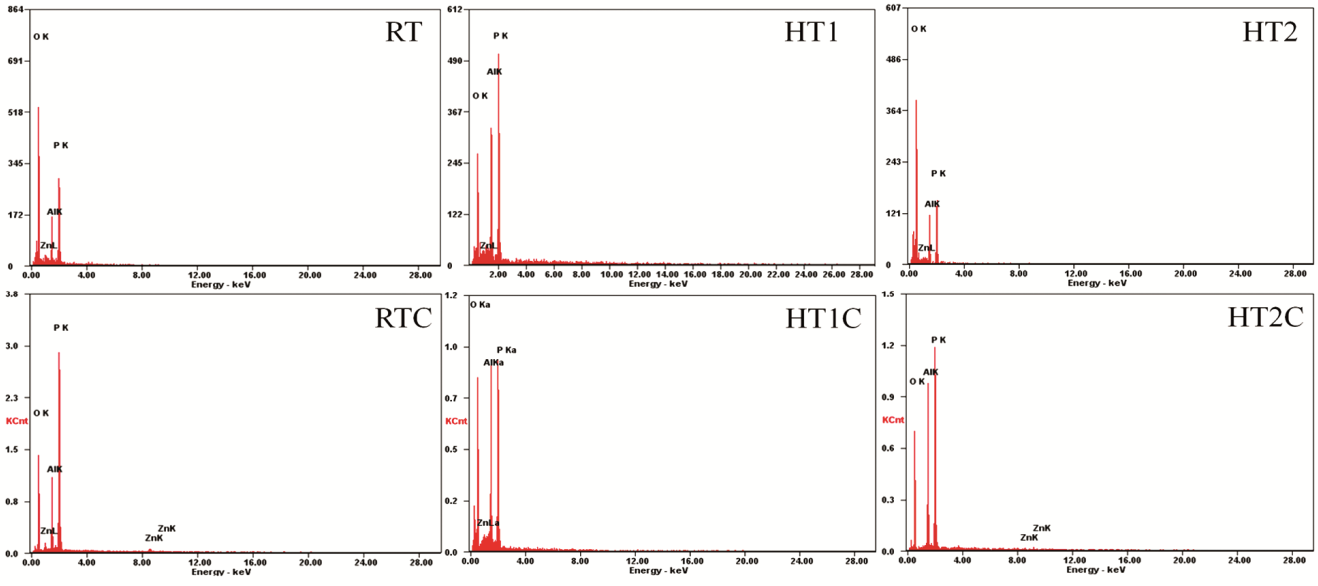

Fig. 3 — EDX analysis of $ZnAlPO_4$ samples

activity towards bi-functional acid catalysis. Hence, this sample (RTC) is tested for its activity towards toluene hydroxylation by using H_2O_2 as an oxidizing agent. The toluene hydroxylation reaction is conducted at 70°C for 4 h, and the reaction products obtained in the conversion of toluene are given in Table 1. A possible mechanism is given in Scheme 1. Here, hydroxylation at aromatic carbon was observed to be the major reaction to produce cresols (85% selectivity) (product A) and 2-methyl-1, 4-benzoquinone (5% selectivity) (product B), which supports the chemo-selective nature of the catalyst. However, a low selectivity for side chain oxidation and hydroxylation products, i.e., benzaldehyde and benzyl alcohol (10% selectivity) (product C+D), was also observed in the product. Among the cresols, para-cresol is the major product (46%) that makes the present process important for pharmaceutical, polymer, and dye industrial applications. Below 70°C, less conversion of toluene is observed; above this temperature, the selectivity of cresol is very low, and reused catalysts also show very good conversion of toluene and selectivity of cresols.

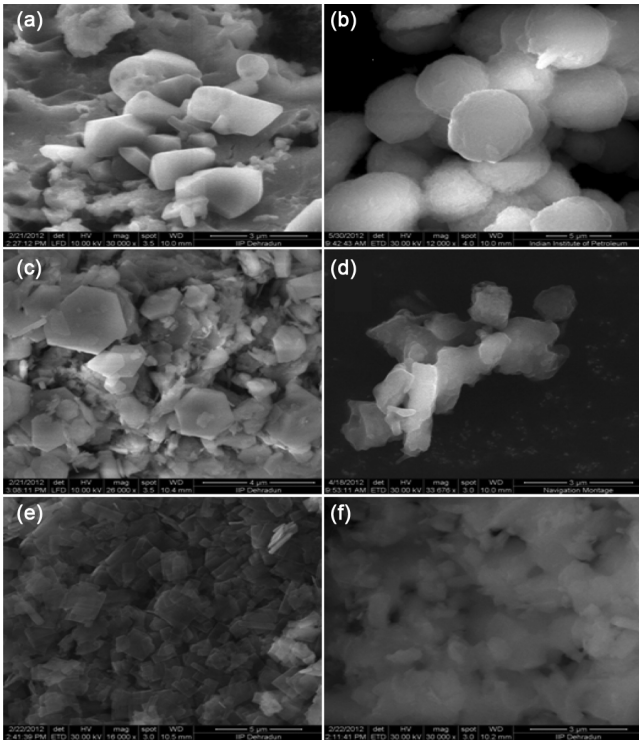

Fig. 4 — SEM images of $ZnAlPO_4$ samples: (a) RT, (b) HT1, (c) HT2, (d) RTC, (e) HT1C and (f) HT2C

Table 1 — Performance of $ZnAlPO_4$ in toluene hydroxylation [a]

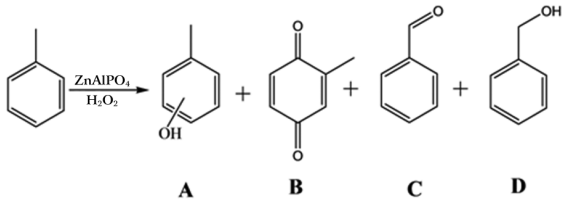

[a] 70°C, 0.8 g Toluene , 1.7 g 50% H_2O_2, 2 mL acetonitrile, 0.16 g catalyst at 4 h

Catalyst	Conversion toluene (%)	Selectivity (%)		
		A	B	C+D
RTC	30	85	5	10
RTC (Recycle)	28	60	10	30

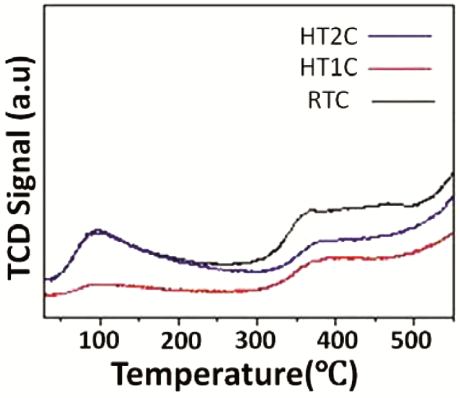

Fig. 5 — TPD spectra of the synthesized $ZnAlPO_4$

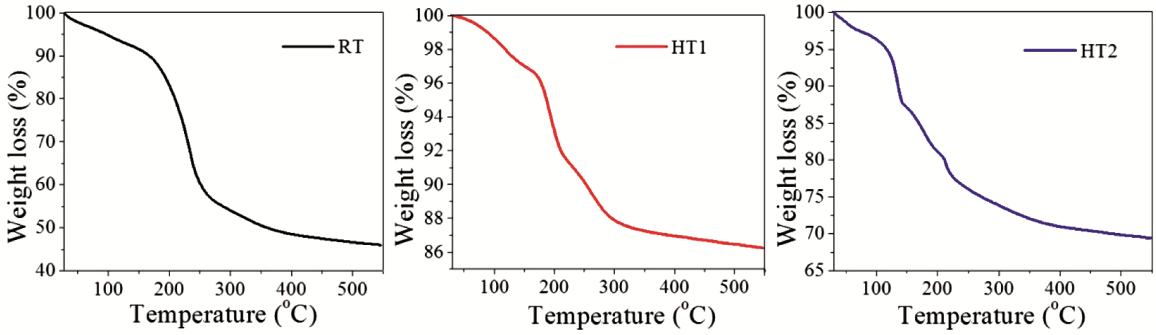

Fig. 6 — TGA plot of the synthesized $ZnAlPO_4$

Table 2 — Various catalytic systems used for hydroxylation of toluene with H_2O_2

S. No	Catalyst	Temperature (°C)	Time (h)	Solvent	Conversion (%)	Selectivity (%)			o and m : p	Ref
						A	C+D	Others		
1	$ZnAlPO_4$(RTC)	70	4	CH_3CN	30	85	10	5(B)	54:46	This work
2	$ZnAlPO_4$ (RTC)(Reused)	70	4	CH_3CN	28	60	30	10(B)	58:42	This work
3	V-$AlPO_4$	80	24	CH_3CN	28.4	21.8	72.5	1	55:45	22
4	Cu-$AlPO_4$	60	3	—	14	69	27	4	72:28	23
5	Cr-$AlPO_4$ [a]	375	—	—	9.19	0	25.3	74.7	0	24
9	V-AlPO-31 [b]	100	22	CH_3CN	—	5	95	0	5:0	25

[a] O_2 oxidizing agent and [b] oxidizing agent TBHP

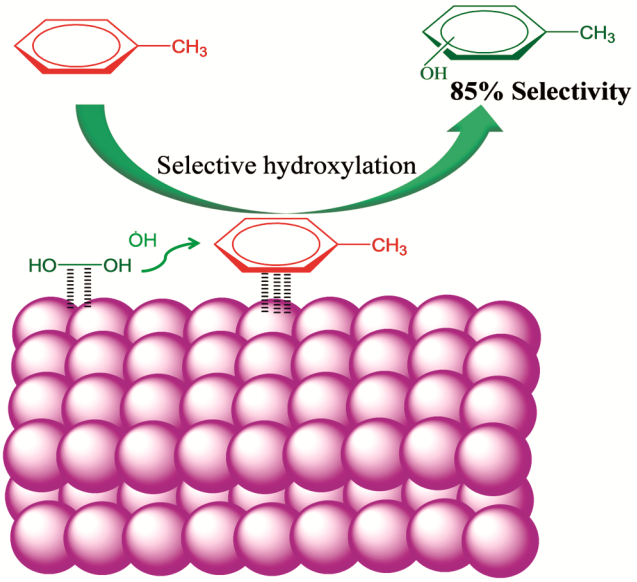

Scheme 1

Though the selective hydroxylation reactions were reported on metal $AlPO_4$ materials earlier, most of the reactions took place at the side chain, and the selective hydroxylation (90%) at the benzene ring of arenes was not observed on such systems (Table 2). We are reporting the chemo-selective nature of $ZnAlPO_4$ (RTC) for the hydroxylation of arenes. This clearly indicated the new type of active sites created in $ZnAlPO_4$ that are responsible for the novel chemo-selective properties of the catalyst for the production of cresol, and the subject is expected to open up new applications of these materials. The preferential polarizability of the C-H in the benzene ring to that of the methyl group in the present study may be due to the strong interaction of $ZnAlPO_4$ with the electron-rich benzene ring. Further, the performance of the $ZnAlPO_4$ catalyst in the present study is observed to be superior to that of the $ZnAlPO_4$-based catalysts reported in the literature[22–25] (Table 2). A reference experiment conducted in the absence of a catalyst, using only H_2O_2, ascertained that no reaction occurred and confirmed the catalytic role of $ZnAlPO_4$. However, the other two samples exhibiting LEV structure (HT1C and HT2C) did not show any catalytic activity, which may be due to the less acidic nature of this phase.

Conclusion

In summary, the present study describes a novel method for the synthesis of LEV and ANA-zeotype nanostructures of $ZnAlPO_4$ materials exhibiting high thermal stability. The synthesis of $ZnAlPO_4$ possessing the ANA-zeotype reported here and the material were also observed to exhibit considerable catalytic activity towards selective hydroxylation of toluene. These findings open up further studies to explore the potentiality of this class of material for various high-temperature applications. The LEV-zeotype nanostructures of $ZnAlPO_4$ obtained in the present study provide a simple synthesis method using a simple organic template, TPABr, with a sorter synthesis time of just 24 h. Moreover, the material retains its structure even after the removal of organic templates through calcination, which further reveals the suitability of these materials for various types of high-temperature applications.

Acknowledgement

Authors are thankful to the INSH-SRMU for providing us this opportunity to carry out the work. They are also thankful to XRD, IR, gas adsorption analysis, and SEM groups at CSIR-IIP for analysis.

References

1 Saadoune I, Cora F & Catlow C R A, Computational study of the structural and electronic properties of dopant ions in microporous AlPOs. 1. Acid catalytic activity of divalent metal ions, *J Phys Chem B*, 107 (2003) 3003.

2 Cheetham A. K, Férey G & Loiseau T, Open-framework inorganic materials, *Angew Chem Int Ed*, 38 (1999) 3268.

3 Flanigen E M, Lok B H, Patton R L & Wilson S T, Aluminophosphate molecular sieves and the periodic table, *Pure Appl Chem*, 58 (1986) 1351.

4 Hortigüela L G, Corà F & Catlow C R A, Mechanism and energetics of secondary oxidation reactions in the aerobic oxidation of hydrocarbons catalyzed by Mn-doped nanoporous aluminophosphates, *J Phys Chem* C, 116 (2012) 6691.

5 Hortigüela L G, Corà F, Sankar G, Wilson C M Z & Catlow C R A, Catalytic reaction mechanism of Mn-doped nanoporous aluminophosphates for the aerobic oxidation of hydrocarbons, *Chem Eur J,* 16 (2010) 13638.

6 Lohse U, Parlitz B, Müller D, Schreier E, Bertram R & Fricke R, MgAPO molecular sieves of CHA and AFI structure — Acidity and Mg ordering, *Micropor Mater*, 12 (1997) 39.

7 Bu X, Feng P & Stucky G D, Novel Germanate zeolite structures with 3-Rings, *J Am Chem Soc*, 120 (1998) 11204.

8 Feng P, Bu X & Stucky G D, Hydrothermal syntheses and structural characterization of zeolite analogue compounds based on cobalt phosphate, *Nature*, 388 (1997) 735.

9 Cavellec M R, Riou D & Ferey G, Magnetic iron phosphates with an open framework, *Inorg Chim Acta*, 291 (1999) 317.

10 Lii K H, Huang Y F, Zima V, Huang C Y, Lin M H, Jiang Y C, Liao F L & Wang S L, Syntheses and structures of organically templated iron phosphates, *Chem Mater*, 10 (1998) 2599.

11 Venkatathri N, Synthesis and NMR characterization of SAPO-35 from non-aqueous systems using hexamethyleneimine template, *Mater Res Bull*, 40 (2005) 1157.

12 Lok B M, Messina C A, Patton R L, Gajek R T, Cannan T R & Flanigen E M, Silicoaluminophosphate molecular sieves: another new class of microporous crystalline inorganic solids, *J Am Chem Soc*, 106 (1984) 6092.

13 Barrett P A & Jones R H, Evidence for ordering of cobalt ions in the microporous solid acid catalyst CoDAF-4 by single crystal X-ray diffraction and resonant X-ray powder diffraction, *Phys Chem Chem Phys*, 2 (2000) 407.

14 Christensen A N & Hazell R G, Use of hydrofluoric acid as Mineralizer in Hydrothermal and Organothermal Synthesis of Me^{2+}-substituted aluminophosphates. I, *Acta Chem Scand*, 53 (1999) 403.

15 Wang Y, Shao L, Li Y, Li X, Li J, Yu J & Xu R, LEV-zeotype magnesium aluminophosphates with variable Mg/Al ratios, *Dalton Trans*, 41 (2012) 6855.

16 Viswanadham N, Sandeep K S & Sreenivasulu P, Facile synthesis of bio-fuel from glycerol over zinc aluminium phosphate nanoplates, *Sust Energy Fuel*, 1 (2017) 1018.

17 Sreenivasulu P, Devaki N, Sreedhar B & Viswanadham N, Room temperature synthesis of $ZnAlPO_4$ nanoparticles and their catalytic applications, *RSC Adv*, 3 (2013) 13651.

18 Sun D L, Deng J R & Chao Z S, Catalysis over zinc-incorporated berlinite ($ZnAlPO_4$) of the methoxycarbonylation of 1,6-hexanediamine with dimethyl carbonate to form dimethylhexane-1,6-dicarbamate, *Chem Cent J*, 1 (2007) 1.

19 Munoz T J, Prakash A, Kevan L & Balkus K J, Synthesis and characterization of CuAPO-5 molecular sieves: Evidence for the framework incorporation of Cu(II) Ions, *J Phys Chem*, 102 (1998) 1379.

20 Pawlig O & Trettin R, In-Situ DRIFT Spectroscopic investigation on the chemical evolution of zinc phosphate acid−base cement, *Chem Mater*, 12 (2000) 1279.

21 Akporiaye D E, Fjellvag H, Halvorsen E N, Hustveit J, Karlsson & Lillerud K P, UiO-7: A new aluminophosphate phase solved by simulated annealing and high-resolution powder diffraction, *J Phys Chem*, 100 (1996) 16641.

22 Subrahmanyam C, Louis B, Viswanathan B, Renken A & Varadarajan T K, Synthesis, characterisation and catalytic properties of vanadium substituted mesoporous aluminophosphates, *Appl Catal A*, 282 (2005) 67.

23 Chou B, Tsai J L & Cheng S, Cu-substituted molecular sieves as liquid phase oxidation catalysts, *Micropor Mesopor Mater*, 48 (2001) 309.

24 Subrahmanyam C, Louis B, Rainone F, Viswanathan B, Renken A & Varadarajan T K, Catalytic oxidation of toluene with molecular oxygen over Cr-substituted mesoporous materials, *Appl Catal A*, 241 (2003) 205.

25 Venkatathri N, Synthesis, characterization and catalytic properties of vanadium aluminophosphate molecular sieves VAPO-31 and VAPSO-Amr from non-aqueous media, *Appl Catal A*, 310 (2006) 31.